Oxysterol-binding protein (OSBP) is required for the perinuclear localization of intra-Golgi v-SNAREs

Taki Nishimura[a,*], Yasunori Uchida[a], Rieko Yachi[a], Tetyana Kudlyk[b], Vladimir Lupashin[b], Takao Inoue[a,†], Tomohiko Taguchi[a,c], and Hiroyuki Arai[a,c]

[a]Department of Health Chemistry and [c]Pathological Cell Biology Laboratory, Graduate School of Pharmaceutical Sciences, University of Tokyo, Tokyo 113-0033, Japan; [b]Department of Physiology and Biophysics, College of Medicine, University of Arkansas for Medical Sciences, Little Rock, AR 72205

ABSTRACT **Oxysterol-binding protein (OSBP) and OSBP-related proteins (ORPs) have been implicated in the distribution of sterols among intracellular organelles. OSBP regulates the Golgi cholesterol level, but how it relates to Golgi function is elusive. Here we report that OSBP is essential for the localization of intra-Golgi soluble vesicle *N*-ethylmaleimide-sensitive fusion attachment protein receptors (v-SNAREs). Depletion of OSBP by small interfering RNA causes mislocalization of intra-Golgi v-SNAREs GS28 and GS15 throughout the cytoplasm without affecting the perinuclear localization of Golgi target-SNARE syntaxin5 and reduces the abundance of a Golgi enzyme, mannosidase II (Man II). GS28 mislocalization and Man II reduction are also induced by cellular cholesterol depletion. Three domains of OSBP—an endoplasmic reticulum–targeting domain, a Golgi-targeting domain, and a sterol-binding domain—are all required for Golgi localization of GS28. Finally, GS28 mislocalization and Man II reduction in OSBP-depleted cells are largely restored by depletion of ArfGAP1, a regulator of the budding of coat protein complex (COP)-I vesicles. From these results, we postulate that Golgi cholesterol level, which is controlled by OSBP, is essential for Golgi localization of intra-Golgi v-SNAREs by ensuring proper COP-I vesicle transport.**

Monitoring Editor
Robert G. Parton
University of Queensland

Received: May 13, 2013
Revised: Aug 22, 2013
Accepted: Sep 10, 2013

INTRODUCTION

Oxysterol-binding protein (OSBP) and OSBP-related proteins (ORP1–11) constitute a large gene family characterized by a C-terminal cholesterol/oxysterol-binding domain (Fairn and McMaster, 2008; Ngo *et al.*, 2010; Raychaudhuri and Prinz, 2010; Vihervaara *et al.*, 2011). They differentially localize to intracellular membranes and the plasma membrane (PM). Recent studies indicate that ORPs play important roles in nonvesicular transport of cholesterol and other sterols among intracellular organelles. Sterol transport between the PM and the endoplasmic reticulum (ER) in yeast is severely compromised when all seven yeast ORPs are missing (Raychaudhuri *et al.*, 2006). Knockdown of ORP5 causes cholesterol accumulation in late endosomes and lysosomes, which is similar to the cholesterol-trafficking defect observed in Niemann–Pick type C fibroblasts (Du *et al.*, 2011). We also showed that ORPs are required for regulating the cholesterol level in late endosomes/lysosomes in *Caenorhabditis elegans* (Kobuna *et al.*, 2010).

OSBP, a founding member of ORP family, was first identified as a cytosolic receptor for oxysterols such as 25-hydroxycholesterol (Taylor *et al.*, 1984; Dawson *et al.*, 1989). OSBP also binds cholesterol and transfers it between liposomes in vitro (Ngo and Ridgway, 2009). In cells, OSBP partitions between the ER and the Golgi (Ridgway *et al.*, 1992) through a "two phenylalanines in an acidic tract" (FFAT) motif that binds vesicle-associated membrane protein–associated

This article was published online ahead of print in MBoC in Press (http://www.molbiolcell.org/cgi/doi/10.1091/mbc.E13-05-0250) on September 18, 2013.

Present addresses: *Department of Biochemistry and Molecular Biology, Graduate School and Faculty of Medicine, University of Tokyo, Tokyo 113-0033, Japan; †Division of Cellular and Gene Therapy Products, National Institute of Health Sciences, Tokyo 158-8501, Japan.

Address correspondence to: Hiroyuki Arai (harai@mol.f.u-tokyo.ac.jp).

Abbreviations used: ACAT, acyl-CoA:cholesterol acyltransferase; Cav1, caveolin-1; COP, coat protein complex; 7-DHC, 7-dehydrocholesterol; FFAT, two phenylalanines in an acidic tract; HMG-CoA, 3-hydroxy-3-methylglutaryl-CoA; LPDS, lipoprotein-deficient serum; Man II, mannosidase II; ORP, OSBP-related protein; OSBP, oxysterol-binding protein; PH, pleckstrin homology; SNARE, soluble *N*-ethylmaleimide-sensitive fusion attachment protein receptor; Syn5, syntaxin5; VAP, vesicle-associated membrane protein–associated protein.

protein (VAP) in the ER (Wyles *et al.*, 2002; Loewen *et al.*, 2003) and a pleckstrin homology (PH) domain that interacts with phosphatidylinositol-4-phosphate (PI4P) in the Golgi (Levine and Munro, 2002). Knockdown of OSBP decreases the Golgi cholesterol level (Banerji *et al.*, 2010). Thus it is proposed that OSBP regulates the transport of cholesterol from the ER to the Golgi.

Cholesterol levels are low in the ER, high in the PM, and intermediate in the Golgi (van Meer, 1989; Mesmin and Maxfield, 2009). Golgi cholesterol has been implicated in Golgi morphology and function. Cholesterol depletion with methyl-β-cyclodextrin (MβCD) condenses GM130 (a *cis*-Golgi protein) and *N*-acetylglucosaminyl transferase I (a *cis*-Golgi protein) to the perinuclear region (Stuven *et al.*, 2003), whereas cholesterol loading disperses GM130 and TGN46 (a *trans*-Golgi network protein) throughout the cytoplasm (Ying *et al.*, 2003). Vesicular stomatitis virus G transport from the Golgi to the PM is inhibited by either cellular cholesterol depletion or cholesterol loading (Stuven *et al.*, 2003; Ying *et al.*, 2003). Membrane rafts, cholesterol-sphingolipid-protein assemblies, have been postulated to function in post-Golgi membrane trafficking and cargo sorting at the *trans*-Golgi network (Simons and Gerl, 2010). In yeast, immunoisolation of post-Golgi vesicles using a raft marker protein as the bait showed that ergosterol, a yeast cholesterol homologue, is selectively enriched in the transport vesicles (Klemm *et al.*, 2009).

The Golgi is a dynamic polarized organelle that receives cargoes from the ER at the *cis* side and moves them to the *trans* side through the medial compartment (Mellman and Warren, 2000). Within the Golgi, the cargoes are modified by glycosidases and glycosyltransferases. These enzymes are nonuniformly distributed within the Golgi stack, allowing sequential modifications of the cargoes (Kornfeld and Kornfeld, 1985). In both yeast and mammalian systems, Golgi enzymes constantly recycle in a retrograde *trans*-to-*cis* manner by means of membrane transport to maintain their abundance and nonuniform distribution (Pelham and Rothman, 2000; Glick and Nakano, 2009). The fusion of recycling transport vesicles with the acceptor membrane requires soluble *N*-ethylmaleimide-sensitive fusion attachment protein receptors (SNAREs), with v-SNAREs on the transport vesicles and target (t)-SNAREs on the acceptor compartment (Sollner *et al.*, 1993).

In the present study, we find that depletion of OSBP dispersed intra-Golgi v-SNAREs (GS28 and GS15) throughout the cytoplasm without affecting the localization of Golgi t-SNARE syntaxin5 (Syn5), reduced the abundance of a Golgi enzyme, mannosidase II (Man II), and mislocalized the γ-subunit of the coat protein complex I (COP-I; γ-COP) from the Golgi, which is a constituent of COP-I vesicles that participates in intra-Golgi transport. The mislocalization of GS28 and the reduction of Man II in OSBP-depleted cells were largely restored by depletion of ArfGAP1, a regulator of the budding of COP-I vesicles. Our results suggest that the Golgi cholesterol level, which is controlled by OSBP, is essential for the Golgi localization of intra-Golgi v-SNAREs by regulating proper COP-I vesicle transport.

RESULTS

Effect of OSBP depletion on Golgi proteins

Because OSBP is primarily associated with the Golgi (Ridgway *et al.*, 1992), we examined the effect of OSBP depletion on the localization and expression of a number of Golgi proteins. OSBP expression was effectively reduced at 72 h after transfection of small interfering RNA (siRNA; OSBP siRNA#1) in HeLa cells (Figure 1A). We did not find much difference in the localization of Golgi proteins, such as *cis*-Golgi protein GM130, *trans*-Golgi proteins p230 and TGN46, Syn5 (Golgi t-SNARE), and VAMP4 (*trans*-Golgi v-SNARE), between control and OSBP siRNA–treated cells (Figure 1B and Supplemental Figure S1A). In addition, overall protein secretion was normal in OSBP-depleted cells (Supplemental Figure S1B). In contrast, OSBP depletion affected intra-Golgi v-SNAREs (GS28 and GS15). These two v-SNAREs lost their compact perinuclear localization and were dispersed throughout the cytoplasm. The GS28 dispersion occurred in >70% of OSBP-depleted cells under the present conditions (Figure 1C). The abundance of GS28 did not change (Figure 1A). GS28 and Syn5 form a v-t SNARE complex (Hay *et al.*, 1997). The amount of coprecipitation between GS28 and Syn5 in OSBP-depleted cells was reduced compared with that in control cells (Figure 1D), consistent with their different localizations. The abundance of Man II was drastically reduced in OSBP-depleted cells (Figure 1A). Treatment with two other OSBP siRNA oligos resulted in the same phenotype of GS28 mislocalization and Man II reduction (Supplemental Figure S2).

OSBP mediates sterol-dependent recruitment of ceramide transfer protein (CERT) to the Golgi, resulting in increased ceramide transfer and sphingomyelin synthesis (Perry and Ridgway, 2006). To test whether the defects in OSBP-depleted cells are due to impaired CERT function, we examined the localization and expression of several Golgi proteins in CERT-depleted cells. CERT was effectively knocked down in cells treated with siRNA#1 and, to a lesser extent, siRNA#2 (Figure 2A). CERT depletion resulted in fragmented or loosely packed distributions of Golgi proteins (GM130, TGN46, GS28, and Syn5) at perinuclear area (Figure 2B). The degree of Golgi fragmentation was correlated with that of CERT depletion (Figure 2, B and C). The expression levels of GS28 and Man II were reduced in CERT-depleted cells (Figure 2A). Thus CERT depletion affected differently the localization and expression of Golgi proteins from OSBP depletion. The overexpression of CERT in OSBP-depleted cells did not restore the mislocalization of GS28 (Figure 2D). These results suggest that mislocalization of Golgi v-SNAREs in OSBP-depleted cells is not due to impaired CERT function.

PH domain, FFAT motif, and sterol-binding domain of OSBP are all necessary for the perinuclear Golgi localization of GS28

OSBP has a PH domain for Golgi targeting, an FFAT motif for ER targeting, a sterol-binding domain, and several phosphorylation sites (Figure 3A). To assess contributions of individual domains to the perinuclear Golgi localization of GS28, we transiently transfected OSBP-depleted cells with Myc-tagged, siRNA-resistant OSBP mutants, including a PI4P-binding–defective mutant (R109/110E; Levine and Munro, 2002), VAP-binding defective mutants (EFFD/ALLA and ΔFFAT; Loewen *et al.*, 2003), phosphorylation-defective (S381A) and phosphorylation mimic (S381/384/387E) mutants (Mohammadi *et al.*, 2001), and a sterol-binding–defective mutant (K495A; Im *et al.*, 2005). Transfection with the siRNA-resistant OSBP wild-type construct (WT*; Figure 3B) fully restored the perinuclear Golgi localization of GS28 (Figure 3, C and D). The PI4P-binding–defective mutant, the VAP-binding–defective mutants, and the sterol-binding–defective mutant of OSBP did not restore the perinuclear localization of GS28. The expression of WT*-OSBP also restored Man II expression in OSBP-depleted cells, but the K495A mutant could not (Supplemental Figure S3). These results showed that these three domains of OSBP are all required for the perinuclear localization of GS28. On the other hand, phosphorylation/dephosphorylation of Ser-381, Ser-384, and Ser-387 of OSBP was dispensable because the perinuclear localization of GS28 was restored by the expression of phosphorylation-defective and mimic mutants.

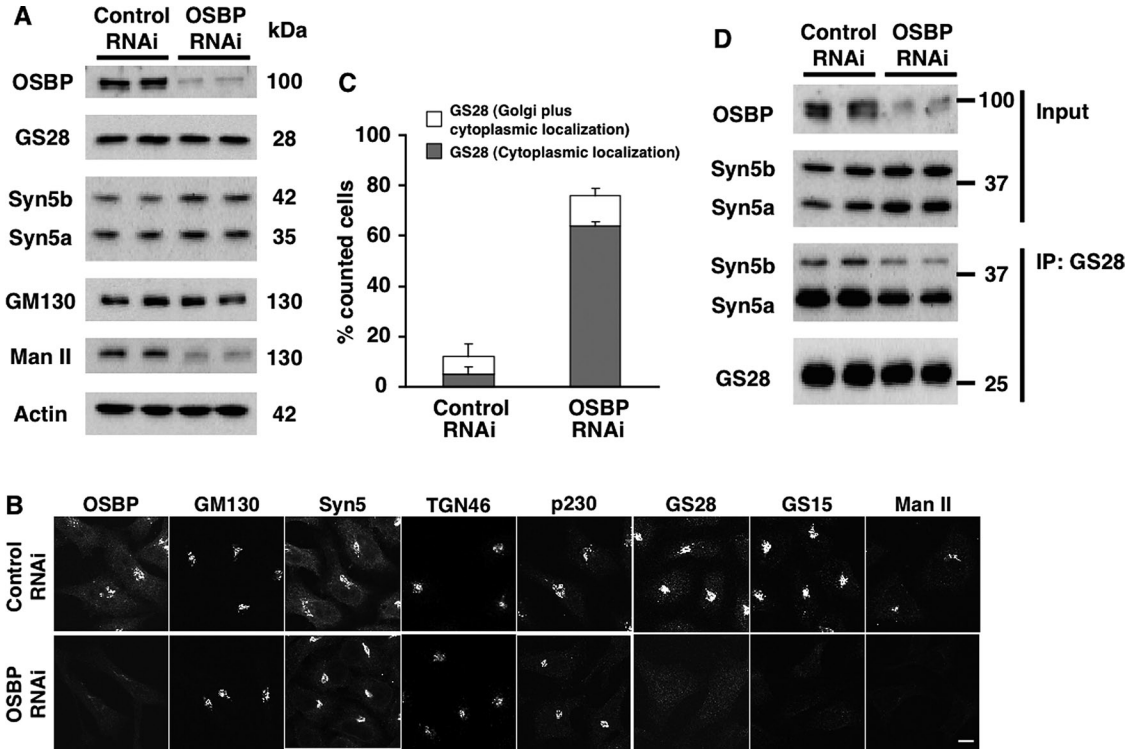

FIGURE 1: OSBP depletion mislocalizes intra-Golgi v-SNAREs (GS28 and GS15) throughout the cytoplasm and reduces the level of Golgi enzyme Man II. HeLa cells were transfected with either control or OSBP siRNA (OSBP siRNA#1). All experiments were performed 72 h after siRNA transfections. (A) Cell lysates were subjected to SDS–PAGE and immunoblotted with the indicated antibodies. (B) Cells were fixed and stained with the indicated antibodies. Scale bar, 10 μm. (C) GS28 localization was examined by immunofluorescence and classified into three categories: 1) perinuclear Golgi localization, 2) Golgi plus cytoplasmic localization, and 3) cytoplasmic localization. More than 40 cells were examined per sample. The data (mean ± SEM) are calculated based on three independent experiments. (D) Coimmunoprecipitation between GS28 and Syn5. Cell lysates were immunoprecipitated with anti-GS28 antibody, and the precipitates were immunoblotted with the indicated antibodies.

OSBP depletion affects cholesterol distribution in ER and Golgi

Ridgway and his colleagues showed biochemically that the cholesterol level of endosome/*trans*-Golgi network decreases in OSBP-depleted cells (Banerji *et al.*, 2010). We took another approach to validate the cholesterol level, using caveolin-1 (Cav1), which accumulates in the Golgi when the cholesterol level in the Golgi is low (Pol *et al.*, 2005; Cubells *et al.*, 2007). In control cells, green fluorescent protein (GFP)–tagged Cav1 (Cav1-GFP) was distributed to the PM and the punctate structures that did not colocalize with GM130 (Figure 4A). In OSBP-depleted cells, Cav1-GFP mostly colocalized with GM130, suggesting that the Golgi cholesterol level is lower than that in control cells. The result provided cell biological evidence that OSBP participates in determining the Golgi cholesterol level. In contrast to OSBP depletion, CERT depletion did not result in Cav1-GFP accumulation at the Golgi (Figure 4B).

Acyl-CoA:cholesterol acyltransferase (ACAT) is present in the ER, and the activity is positively correlated with the cholesterol concentration in the ER (Lange and Steck, 1997). ACAT activity, as measured by the rate of incorporation of [^{14}C]oleic acid to cholesteryl esters (Goldstein *et al.*, 1983), was increased by 1.5-fold in OSBP-depleted cells (Figure 4C), suggesting an increase in cholesterol level in the ER. These results, together with the previous findings, indicate that OSBP is involved in the transport of cholesterol from the ER to the Golgi membrane. The finding that the sterol-binding defective mutant (K495A) did not restore the defect in OSBP-depleted cells (Figure 3, C and D) also support this notion.

Effect of cellular cholesterol depletion on Golgi v-SNAREs and Man II

We then assessed the contribution of cholesterol to the localization and expression of Golgi proteins. Cells were treated for 24 h with lipoprotein-deficient serum (LPDS) plus lovastatin, an inhibitor of 3-hydroxy-3-methylglutaryl-CoA (HMG-CoA) reductase. With this treatment, GS28 was significantly dispersed as OSBP knockdown (Supplemental Figure S4, A and B). Syn5 remained at the perinuclear region, with a slightly dispersed pattern. Because lovastatin affects biosynthesis of dolichol, ubiquinone, and prenylated proteins besides cholesterol biosynthesis, we then used AY9944, a specific inhibitor of 3β-hydroxysterol Δ^7-reductase that catalyzes the conversion of 7-dehydrocholesterol (7-DHC) to cholesterol (Incardona and Roelink, 2000). Cells were treated for 48 h with LPDS plus 5 μM AY9944. This treatment reduced cellular cholesterol to ~35% compared with untreated cells (Figure 5A). Cholesterol depletion with AY9944 dispersed GS28 and GS15 (Figure 5B) and reduced the level of Man II (Figure 5C). Other Golgi proteins (GM130, Syn5, and p230) remained at the perinuclear region (Figure 5B). The interaction of GS28 and Syn5 was also reduced (Figure 5D). These phenotypes are quite similar to those in cells depleted of OSBP. AY9944 treatment caused a

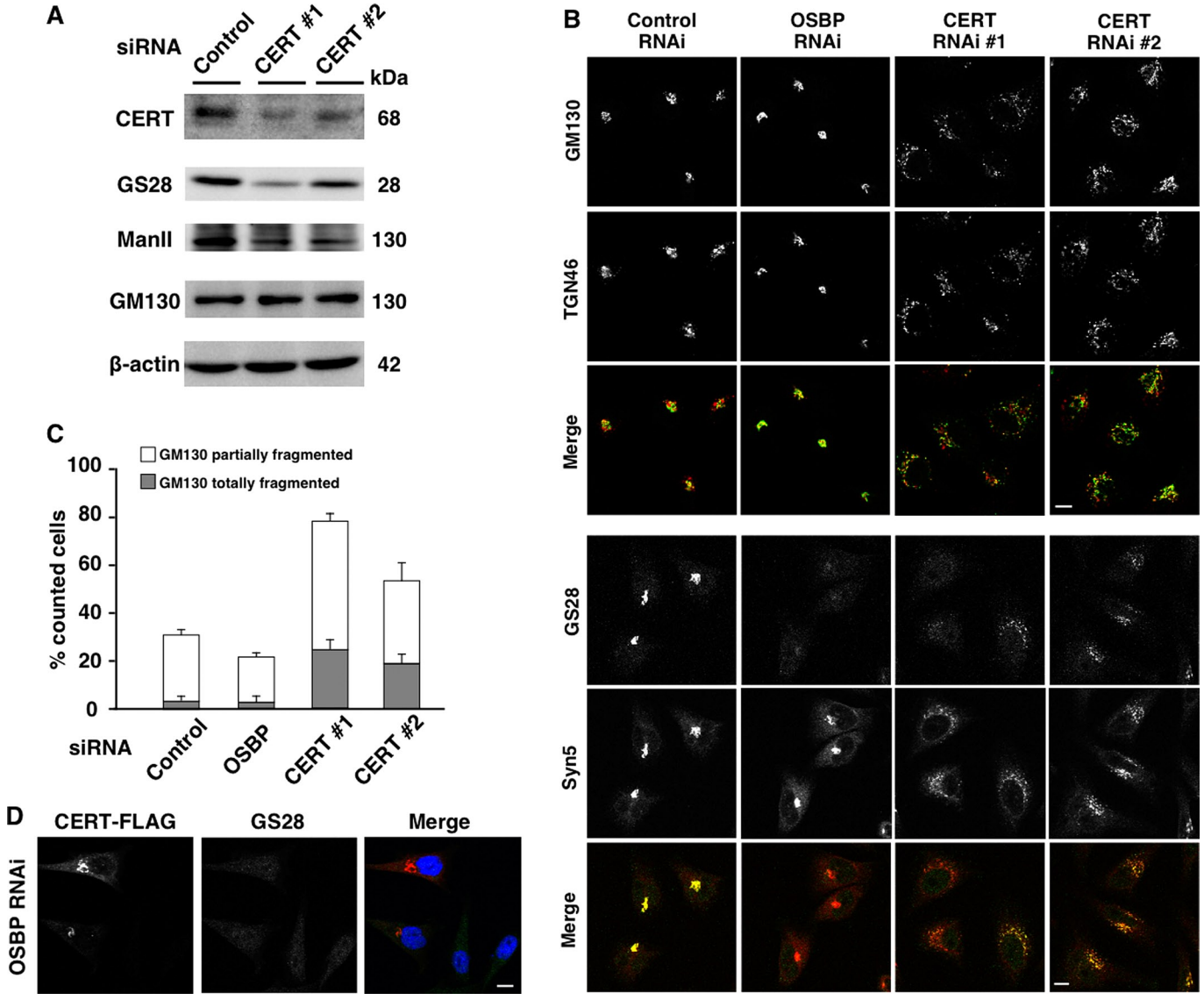

FIGURE 2: CERT depletion induces Golgi fragmentation. HeLa cells were transfected with the indicated siRNAs for 72 h. (A) Cell lysates were subjected to SDS–PAGE and immunoblotted with the indicated antibodies. (B) Cells were fixed and stained with anti-GM130 (green) and anti-TGN46 (red) antibodies, or anti-GS28 (green) and anti-Syn5 (red) antibodies. Scale bar, 10 μm. (C) GM130 localization was examined by immunofluorescence, and percentage of cells with partially or totally fragmented GM130 staining was determined. More than 40 cells were examined per sample. The data (mean ± SEM) are calculated based on three independent experiments. (D) HeLa cells were transfected with OSBP siRNA#1 for 48 h, followed by transfection with the FLAG-tagged CERT plasmid. Seventy-two hours after siRNA transfection, cells were fixed and stained with anti-GS28 (green) and anti-FLAG (red) antibodies. DNA was stained with DAPI (blue). Scale bar, 10 μm.

significant accumulation of 7-DHC in the cells (Figure 5A), but addition of 7-DHC to cells had no effect on GS28 localization (unpublished data).

Implication of COP-I–mediated transport in GS28 dispersion induced by OSBP depletion

Given that GS28 and GS15 are enriched in COP-I–coated vesicles budded from the Golgi (Nagahama *et al.*, 1996; Xu *et al.*, 2002; Yang *et al.*, 2006), we asked whether COP-I is involved in GS28 mislocalization. γ-COP, a subunit of COP-I coat, localized mainly at the Golgi in control cells (Figure 6A). In contrast, γ-COP redistributed drastically from the Golgi to the cytoplasm in OSBP-depleted cells (Figure 6A and Supplemental Figure S5A).

COP-I–mediated transport can be suppressed by depletion of ArfGAP1, a key regulator of the budding process of COP-I vesicles from the Golgi (Lanoix *et al.*, 2001; Yang *et al.*, 2002; Asp *et al.*, 2009). Simultaneous depletion of ArfGAP1 and OSBP largely restored the perinuclear Golgi localization of GS28, being colocalized with Syn5 (Figure 6B–D). The level of Man II was also partly restored in these cells (Figure 6B). In contrast, ArfGAP1 depletion alone did not affect GS28 localization or Man II expression.

These results, together with the observation that γ-COP is mislocalized from the Golgi by OSBP depletion, suggest that COP-I–mediated transport underlies the mislocalization of GS28 and reduction of Man II in OSBP-depleted cells. GS28 did not colocalize with γ-COP in OSBP-depleted cells (Supplemental Figure S5A). This may

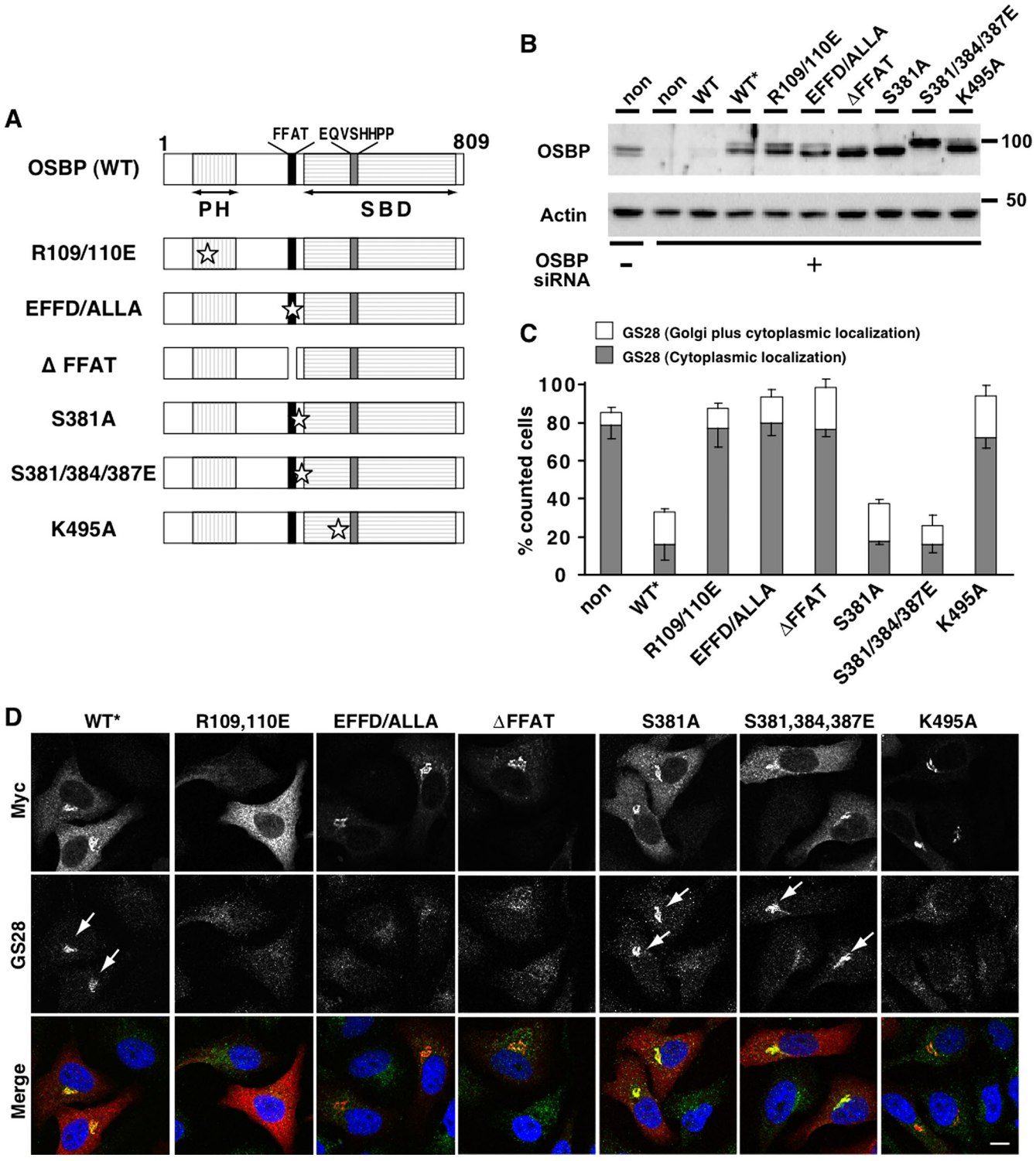

FIGURE 3: PH domain, FFAT motif, and sterol-binding domain of OSBP are necessary for perinuclear localization of GS28. (A) Schematic representations of the wild-type (WT) OSBP and OSBP mutants. EQVSHHPP, OSBP signature motif; FFAT, two phenylalanines in an acidic tract motif; SBD, sterol-binding domain. Stars indicate the site of the mutation introduced. (B) HeLa cells were transfected with control or OSBP#1 siRNA for 48 h, followed by transfection with the indicated plasmids encoding Myc-tagged OSBP or OSBP mutants that contain silent mutations within the siRNA targeting sequence. Seventy-two hours after siRNA transfection, cell lysates were subjected to SDS–PAGE and immunoblotted with anti-OSBP antibody. Transfection with the siRNA-resistant OSBP construct (WT*) increased OSBP expression close to the normal level. (C, D) Cells were transfected with OSBP#1 siRNA for 48 h, followed by transfection with the indicated plasmids encoding siRNA-resistant OSBP mutants. Seventy-two hours after siRNA transfection, cells were fixed and stained with anti-GS28 (green) and anti-Myc (red) antibodies. DNA was stained with DAPI (blue). GS28 localization was quantified (C) as in Figure 1C, and representative images are shown (D). Arrows indicate cells with restored perinuclear localization of GS28 by the expression of WT*, S381A, or S381/384/387E mutants. Scale bar, 10 μm.

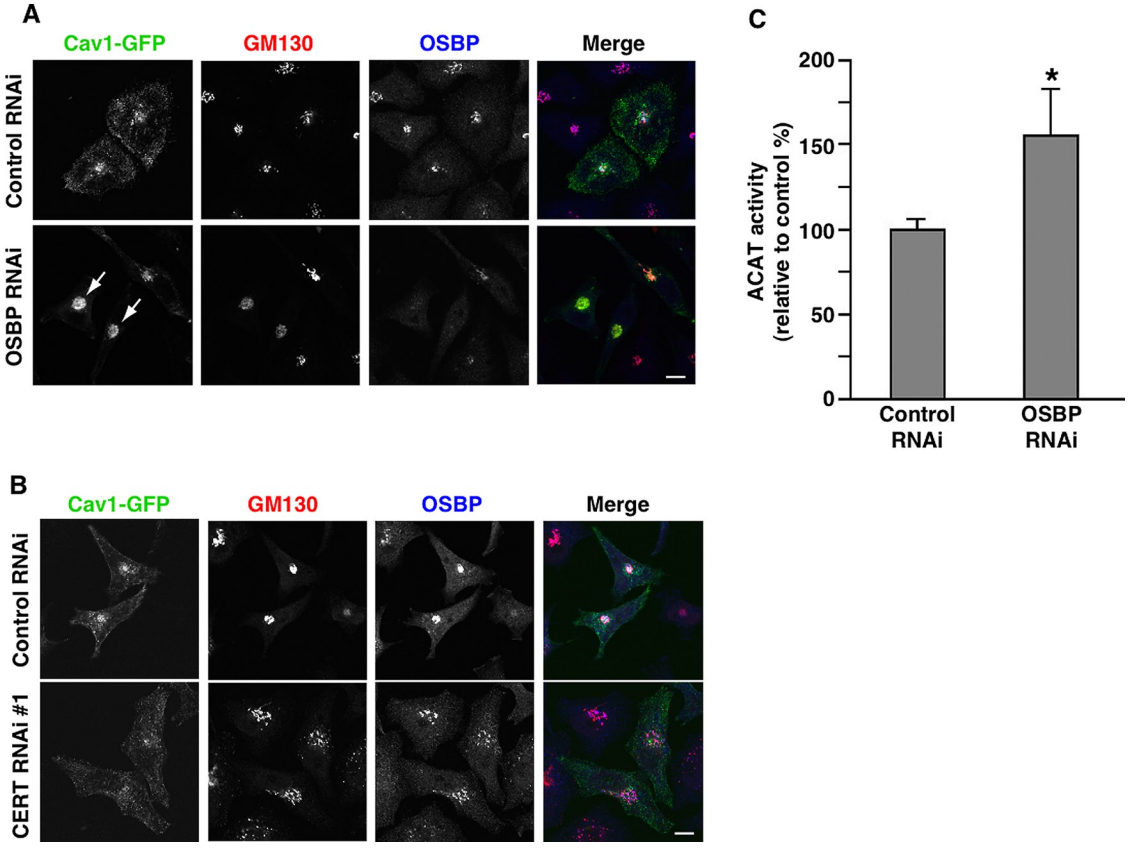

FIGURE 4: Effect of OSBP depletion on Cav1-GFP localization and ACAT activity. (A) HeLa cells were transfected with control or OSBP#1 siRNA for 48 h, followed by transfection with the Cav1-GFP plasmid. Seventy-two hours after siRNA transfection, cells were fixed and stained with anti-GM130 (red) and anti-OSBP (blue) antibodies. Arrows indicate Cav1-GFP accumulation in the Golgi of OSBP-depleted cells. Scale bar, 10 μm. (B) HeLa cells were transfected with control or CERT siRNA#1 for 48 h, followed by transfection with the Cav1-GFP plasmid. Seventy-two hours after siRNA transfection, cells were fixed and stained with anti-GM130 (red) and anti-OSBP (blue) antibodies. Scale bar, 10 μm. (C) Cells were transfected with control or OSBP#1 siRNA. Seventy-two hours after transfection, the rate of cholesterol esterification in the cells was determined. Data represent mean ± SEM (n = 4). *$p < 0.05$ vs. control RNA interference.

be because COP-I coat proteins were uncoated from COP-I vesicles before the fusion of the vesicles to the acceptor Golgi membranes (Tanigawa *et al.*, 1993). The mislocalized GS28 did not colocalize with the ER protein calnexin (Supplemental Figure S5B), indicating that GS28 was not mistargeted to the ER by OSBP depletion.

DISCUSSION

In the present study, we demonstrate that OSBP is essential for the perinuclear Golgi localization of GS28 and GS15, two v-SNAREs involved in intra-Golgi transport. OSBP has an FFAT motif for targeting the ER through the interaction with VAPs, a PH domain for targeting the Golgi membranes through the interaction with PI4P in the Golgi, and a sterol-binding domain. We showed that these three domains in OSBP are all required for the perinuclear Golgi localization of GS28, suggesting that OSBP-dependent cholesterol transport from the ER to the Golgi is required for the Golgi localization of GS28. In addition to these domains, phosphorylation of Ser-381/384/387 of OSBP is reported to be linked to its Golgi localization (Mohammadi *et al.*, 2001). Because both phosphorylation-defective and mimic mutants restored the perinuclear localization of GS28 in OSBP-depleted cells, phosphorylation and dephosphorylation of these serines appear not to be involved in the Golgi v-SNARE localization. This phosphorylation site was recently extended to include Thr-379, Ser-388, and Ser-391, and an additional cluster of phosphoserine residues (Ser-192/195/200) was identified (Goto *et al.*, 2012). Whether the newly identified phosphorylations of OSBP are involved in the Golgi v-SNARE localization needs further investigation.

OSBP participates in the recruitment of CERT from the ER to the Golgi and thereby up-regulation of sphingomyelin synthesis in the Golgi (Perry and Ridgway, 2006). CERT depletion causes the fragmentation of the Golgi, which is consistent with a previous report (Perry and Ridgway, 2006), but did not induce specific mislocalization of Golgi v-SNAREs. Furthermore, overexpression of CERT in OSBP-depleted cells did not restore the mislocalization of GS28. Thus the influence on the Golgi v-SNAREs is selectively attributable to OSBP function, not to CERT function. This function of OSBP is most likely executed by the Golgi cholesterol that is regulated by OSBP, not by the Golgi sphingolipids. The contribution of cholesterol to the GS28 localization was also supported by cellular cholesterol depletion experiment with lovastatin, an inhibitor of HMG-CoA reductase, or with AY9944, an inhibitor of 3β-hydroxysterol Δ^7-reductase.

There is increasing evidence that cholesterol facilitates membrane fusion (Lang *et al.*, 2001; Stuven *et al.*, 2003; Churchward *et al.*, 2005; Linetti *et al.*, 2010). For example, it was suggested that removal of cholesterol from Golgi membrane by use of MβCD inhibits the fusion step of intra-Golgi transport in a cell-free assay (Stuven

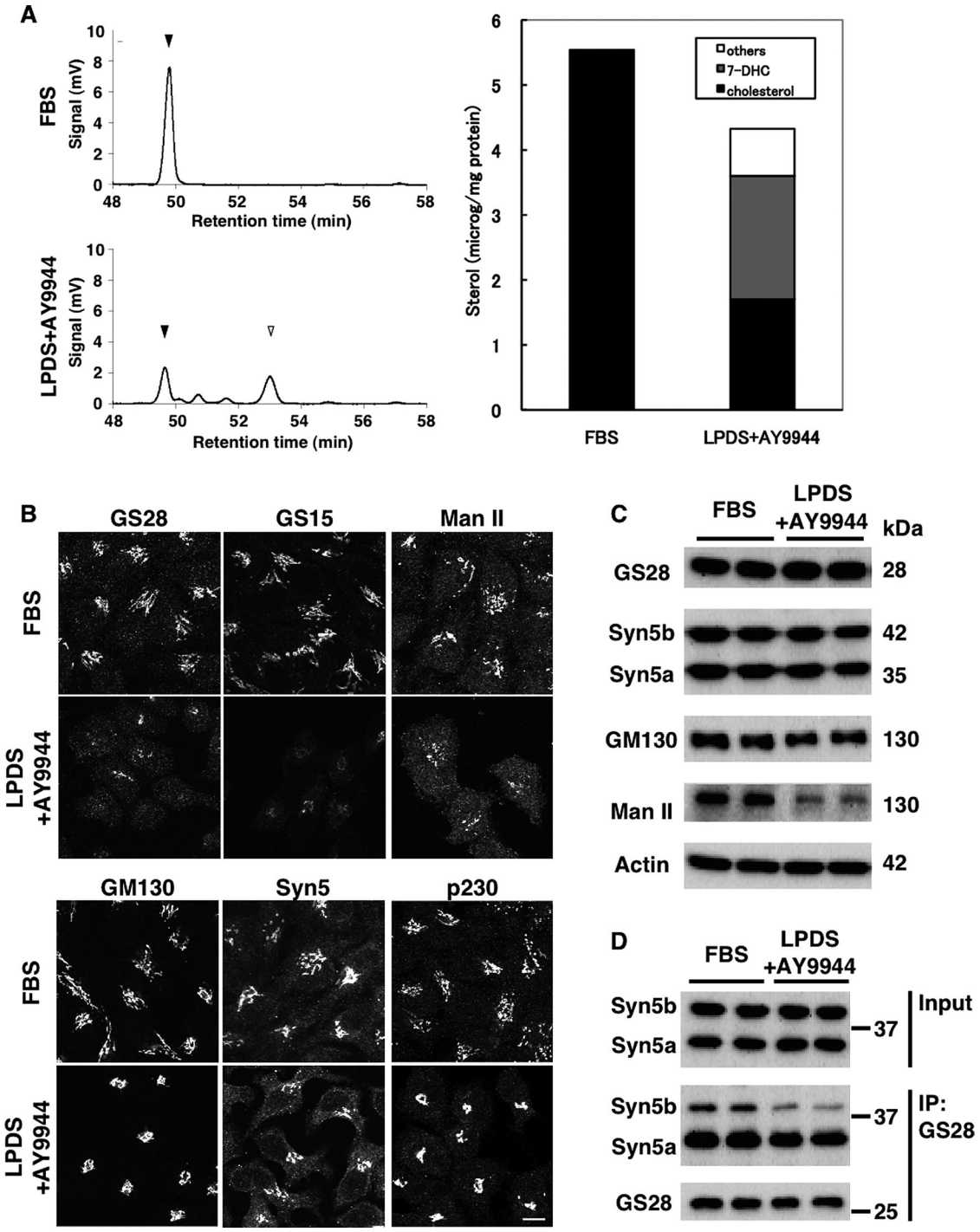

FIGURE 5: Cellular cholesterol depletion mislocalizes intra-Golgi v-SNAREs (GS28 and GS15) throughout the cytoplasm. HeLa cells were grown in medium containing 10% FBS or 5% LPDS plus 5 μM AY9944 for 48 h. (A) Lipids extracted from the cells were analyzed by gas chromatography. The solid and open arrowheads indicate the peak position of cholesterol and 7-DHC, respectively. Total cholesterol (black), 7-DHC (gray), and other lipids (white) in the cells were quantified. Note the accumulation of 7-DHC in LPDS/AY9944-treated cells, which is the immediate precursor of cholesterol. (B) Cells were fixed and stained with the indicated antibodies. Scale bar, 10 μm. (C) Cell lysates were subjected to SDS–PAGE and immunoblotted with the indicated antibodies. (D) Cell lysates were immunoprecipitated with anti-GS28 antibody, and the precipitates were immunoblotted with the indicated antibodies.

et al., 2003). Syntaxin1, a t-SNARE, is concentrated in large, 200-nm cholesterol-dependent clusters at the PM in PC12 cells (Lang *et al.*, 2001). These clusters define docking and fusion sites for secretory vesicles, which suggests that a lateral clustering of transmembrane domains of t-SNARE by cholesterol is required for efficient fusion. By using reconstituted proteoliposomes, it was shown that cholesterol induces a conformational change of the v-SNARE (VAMP2) transmembrane domain from an open scissors-like dimer to a parallel dimer (Tong *et al.*, 2009), which might give VAMP2 a more favorable shape for subsequent membrane fusion. Therefore, one possible

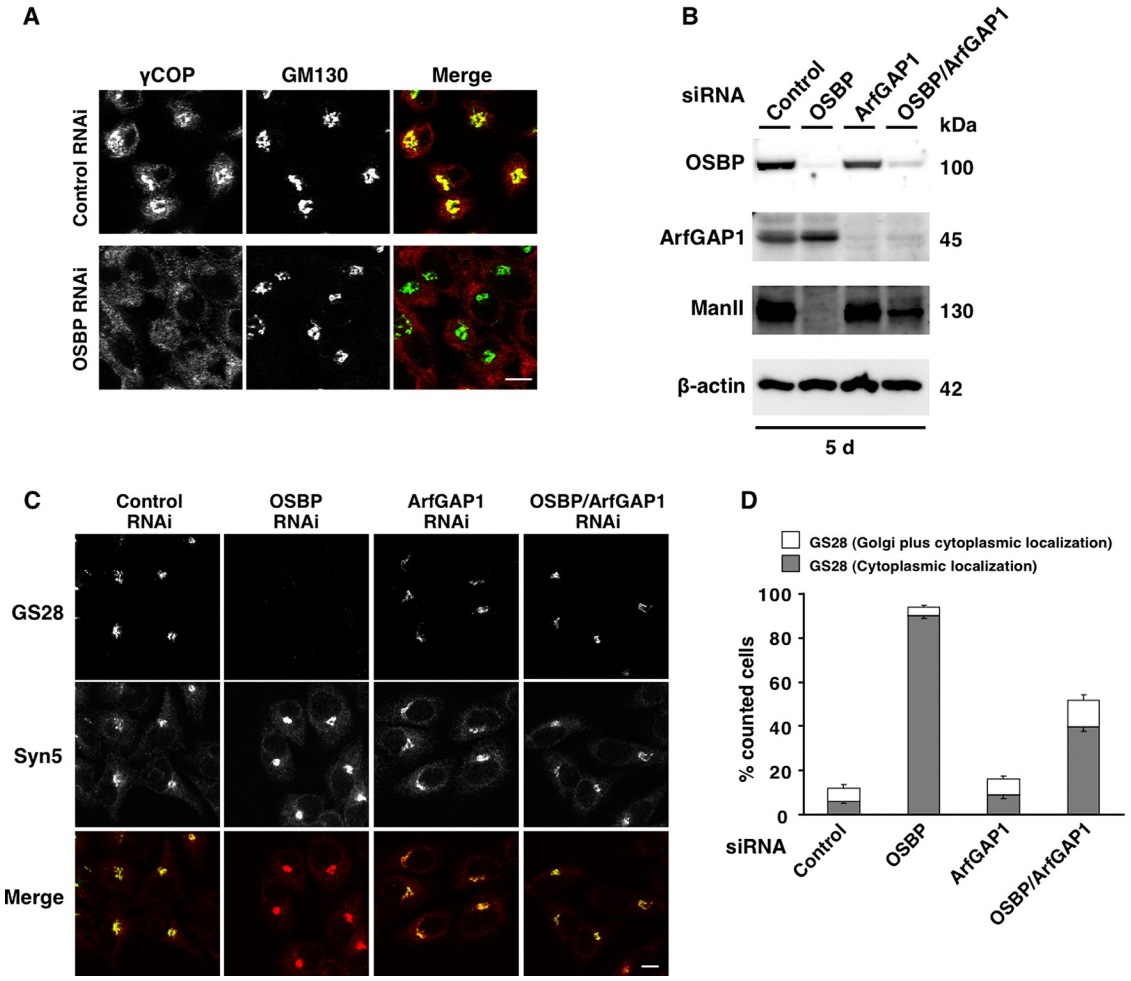

FIGURE 6: Involvement of COP-I–mediated transport in GS28 mislocalization. (A) HeLa cells were transfected with the indicated siRNAs for 72 h. Cells were fixed and stained with anti-GM130 (green) and anti-γ-COP (red) antibodies. Scale bar, 10 μm. (B–D) Simultaneous depletion of ArfGAP1 and OSBP suppresses the GS28 dispersion induced by depletion of OSBP alone. HeLa cells were transfected with the indicated siRNAs twice. The subsequent experiments were performed 5 d after the first siRNA transfection. (B) Cell lysates were subjected to SDS–PAGE and immunoblotted with the indicated antibodies. (C, D) Cells were fixed and stained with anti-GS28 (green) and anti-Syn5 (red) antibodies (C), and the GS28 localization was quantified (D) as in Figure 1C. Scale bar, 10 μm.

scenario is that SNARE activity is lowered in a cholesterol-poor environment in OSBP-depleted cells, which prevents efficient fusion of v-SNARE–containing vesicles to the Golgi. The vesicles that fail to fuse with the Golgi may be eventually dispersed to the cytoplasm.

Of interest, the depletion of OSBP mislocalized not only intra-Golgi SNAREs but also γ-COP, a subunit of COP-I coat, from the Golgi to the cytoplasm. The depletion of ArfGAP1, a key regulator of the budding process of COP-I vesicles from the Golgi, restored the perinuclear Golgi localization of GS28 in OSBP-depleted cells. Thus COP-I–mediated transport may participate in the mislocalization of intra-Golgi SNAREs. As discussed earlier, inefficient fusion of COP-I vesicles to the Golgi because of the lowered SNARE activity would underlie the dispersion of GS28, GS15, and γ-COP. Of note, similar abnormalities, such as mislocalization of intra-Golgi v-SNAREs and COP-I coat from the Golgi to the cytoplasm, reduction of GS28 and Syn5 interaction, and degradation of Golgi enzymes, have been observed in cells depleted of the COG (conserved oligomeric Golgi) complex, an essential tethering factor of COP-I vesicles to the acceptor Golgi membranes (Oka *et al.*, 2004; Zolov and Lupashin, 2005; Shestakova *et al.*, 2007).

In cells treated with AY9944, 7-DHC, a substrate of 3β-hydroxysterol Δ^7-reductase, accumulated with a concomitant decrease of cholesterol. Although 7-DHC differs from cholesterol only in a double bond at the seventh position and is indistinguishable from cholesterol in its ability to become incorporated into membrane rafts, the protein composition of rafts purified from AY9944-treated rat brain tissue is altered (Keller *et al.*, 2004). The altered Golgi raft proteins in AY9944-treated cells might be causative of the mislocalization of v-SNAREs and the reduction of Man II. Of note, deficiency of 3β-hydroxysterol Δ^7-reductase causes Smith-Lemli-Opitz syndrome (SLOS), an autosomal recessive congenital developmental condition that includes such disorders as microcephaly and polydactyly (Porter and Herman, 2011). It is worth examining whether impaired COP-I vesicle transport and/or reduction of Golgi enzymes contribute to the etiology of SLOS.

MATERIALS AND METHODS

Reagents

Leupeptin, aprotinin, pepstatin A, brefeldin A, cholesterol, 7-DHC, lovastatin, AY9944, and 5α-cholestane were purchased from

Sigma (St. Louis, MO). Phenylmethylsulfonyl fluoride was from Wako (Osaka, Japan). Protein G Sepharose 4 Fast Flow was from GE Healthcare (Little Chalfont, UK). [^{35}S]methionine was from Perkin Elmer-Cetus (Waltham, MA). LPDS (d > 1.215 g/ml) was prepared from fetal bovine serum (FBS; purchased from Biowest [Nuaillé, France]) by ultracentrifugation in KBr at a density of 1.215 g/ml. After centrifugation for 45 h at 18°C using a Beckman 45 Ti rotor at 138,000 × g, the lipoprotein layer was removed and the bottom fraction was dialyzed (MWCO 3500; Spectrum Laboratories [Rancho Dominguez, CA]) against phosphate-buffered saline (PBS).

Antibodies

Rabbit polyclonal antibodies were anti-Man II from Chemicon (Billerica, MA) or US Bio (Salem, MA); anti-Myc tag from Upstate (Billerica, MA); anti-Syn5 from Synaptic Systems (Goettingen, Germany); anti-CERT from Bethyl Laboratories (Montgomery, TX); and anti-ArfGAP1 from Abgent (San Diego, CA); anti-OSBP was described previously (Nishimura *et al*., 2005); anti–γ-COP was a kind gift from Rainer Duden (University of Lübeck, Lübeck, Germany). Mouse monoclonal antibodies were anti-GS28, anti-GM130, anti-p230, anti-GS15, anti-calnexin from BD Transduction (San Jose, CA); anti-Syn5 (1C5), a kind gift from Kei Suga and Kimio Akagawa (Kyorin University School of Medicine, Tokyo, Japan); anti-Myc tag (9E10), anti-actin (AC-40), and anti–α-tubulin (DM 1A) from Sigma; and anti–β-actin from Abcam (Cambridge, UK). Sheep polyclonal antibody was anti-TGN46 from Serotec (Hercules, CA). Secondary anti-rabbit immunoglobulin G (IgG)–horseradish peroxidase (HRP) and anti-mouse IgG-HRP were from GE Healthcare. Anti-rat IgG-HRP was from American Qualex (San Clemente, CA).

Cell culture

HeLa cells were maintained in DMEM (Invitrogen, Carlsbad, CA) supplemented with 10% FBS and penicillin-streptomycin-glutamine (GIBCO, Carlsbad, CA) in a 5% CO_2 humidified 37°C cell culture incubator.

RNA interference

siRNA duplexes were synthesized by Nippon Gene (Tokyo, Japan). siRNA sequences are as follows:

OSBP#1: sense, 5′-UACUGGGAGUGUAAAGAAATT-3′; antisense, 5′-UUUCUUUACACUCCCAGUATT-3′

OSBP#2: sense, 5′-CGAACGAGCCACACUCUUUAG-3′; antisense, 5′-AAAGAGUGUGGCUCGUUCGUU-3′

OSBP#3: sense, 5′-GCGAAAUUGAUAUUGUGAAUC-3′; antisense, 5′-UUCACAAUAUCAAUUUCGCCA-3′

ArfGAP1: sense, 5′-GAACCAGGAAGGUUCUUAAAG-3′; antisense, 5′-UUAAGAACCUUCCUGGUUCUU-3′

CERT#2: sense, 5′-CAUCACACCUCACGAUUUUGA-3′; antisense, 5′- AAAAUCGUGAGGUGUGAUGAC-3′

CERT#1 was purchased from Invitrogen (Stealth RNAi, HSS115328). Control siRNA was purchased from Nippon Gene and used as a negative control. For RNA interference, cells were transfected with 20 nM specific siRNAs using Lipofectamine 2000 or Lipofectamine RNAiMAX according to the instructions of the manufacturer (Invitrogen). Forty-eight hours after siRNA transfection, if necessary, plasmids were additionally transfected by using Optifect Reagent according to the instructions of the manufacturer (Invitrogen). Unless indicated otherwise, all the subsequent experiments were performed 72 h after siRNA transfections.

cDNA constructs

Rabbit OSBP (GenBank Accession No. J05056) was obtained from ATCC and subcloned into pcDNA3-Myc vector. To generate siRNA-resistant OSBP (pcDNA3-Myc-OSBP*), six silent mutations (underlined) were introduced into the OSBP siRNA#1 target sequence (AGTATTGGGAATGCAAGGAGA) by PCR. OSBP mutants (R109/110E, EFFD/ALLA, ΔFFAT, S381A, S381/384/387E, and K495A) with siRNA-resistant mutations were generated by using pcDNA3-Myc-OSBP* as a template and subcloned into pcDNA3-Myc. Human caveolin-1 (GenBank Accession No. NM_001753) cDNA was obtained by reverse transcriptase-PCR from total RNA of HeLa cells and subcloned into pEGFP-N3 vector. Human VAMP4 (GenBank Accession No. NM_003762) and human CERT cDNAs (GenBank Accession No. NM_031361) were obtained by reverse transcriptase-PCR from total RNA of HeLa cells and subcloned into pcDNA3-Myc or p3xFLAG-CMV-14 vector.

Lipid extraction

Lipid was extracted according to the Bligh and Dyer method (Bligh and Dyer, 1959). In brief, 800 μl of cell lysates was collected into screw-capped glass tubes. Three milliliters of chloroform-methanol mixture (1:2 [vol/vol]) was added, and the mixture was shaken vigorously for 10 min, and then 1 ml of chloroform and 1 ml of 0.9% KCl were added. The mixture was shaken vigorously again for 10 min, and the phases were separated by centrifugation at 2000 × g for 5 min at room temperature. The chloroform phase (lower layer) was collected and used for subsequent experiments.

Gas chromatography analysis

Extracted lipids were saponified at 60°C for 1 h in ethanolic KOH solution, and unsaponifiable lipids (extracted with hexane) were treated with a mixture of trimethylchlorosilane, 1,1,1,3,3,3-hexamethyldisilazane, and dried pyridine (1:3:9 [vol:vol:vol]) for 30 min at room temperature. The trimethylsilyl derivatives were subjected to gas chromatography analysis, using a model GS353B gas chromatograph (GL Sciences, Tokyo, Japan) equipped with a SPELCO SPB-1TM capillary column (10.25 mm × 60 m, 0.25-mm film thickness; Sigma). The oven temperature was programmed to hold at 50°C for 10 min and then rise to 280°C. The injector and detector temperatures were 300°C. The data were processed using Chromato-PRO (Run Time Corporation, Kanagawa, Japan) and normalized to the signal from the internal standard (5α-cholestane) and total cell proteins. Values were expressed as a percentage of the control. Retention times for cholesterol and 7-DHC were established with synthetic standards.

Immunofluorescence and confocal microscopy

All immunofluorescence steps were performed at room temperature, and cells were extensively rinsed with PBS after each step. HeLa cells grown on poly-L-lysine–coated glass coverslips were fixed with either methanol (–20°C for 10 min) or 3.7% formaldehyde (room temperature for 20 min) in PBS. Formaldehyde-fixed cells were then quenched with 50 mM NH_4Cl in PBS for 10 min and permeabilized with either 0.5% Triton X-100 (vol/vol) for 15 min or 0.1% saponin (wt/vol) for 10 min at room temperature. The cells were blocked with 3% bovine serum albumin (BSA; Sigma) in PBS for 30 min, incubated with the primary antibodies in the same buffer, and visualized with the secondary antibodies conjugated to Alexa dyes (Molecular Probes). We used 4′,6′-diamidino-2-phenylindole (DAPI; Sigma) to stain nuclei. Confocal images were acquired at room temperature on a laser-scanning microscope (LSM510; Carl Zeiss, Oberkochen, Germany) with a 63 × 1.4 plan-Apochromat oil immersion lens using argon and HeNe

lasers or a confocal laser microscope (FV1000D IX81; Olympus, Tokyo, Japan) using a 60× PlanApoN oil immersion lens (1.42 numerical aperture; Olympus). For final output, images were processed using Photoshop 7.0 software (Adobe, San Jose, CA).

Immunoblotting

Cell lysates were subjected to SDS–PAGE and transferred to nitrocellulose or polyvinylidene fluoride membranes using the Bio-Rad protein transfer system. The membranes were blocked with 5% skim milk in Tris-buffered saline containing 0.05% Tween 20 or 1% BSA in PBS and then incubated with the indicated antibodies. Proteins bound to the antibodies were visualized with an enhanced chemiluminescence kit (ECL; Amersham Biosciences, Little Chalfont, UK). For final output, images were processed using Photoshop 7.0 software.

Immunoprecipitation

Cells were collected in ice-cold PBS by scraping and precipitated by centrifugation at 1000 × *g* for 3 min. Precipitated cells were suspended with 500 µl of immunoprecipitation (IP) buffer (20 mM Tris-HCl, pH 7.4, 150 mM NaCl, 1 mM sodium orthovanadate, 50 mM sodium fluoride, 5 µg/ml leupeptin, 5 µg/ml pepstatin A, 5 µg/ml aprotinin, and 1 mM phenylmethylsulfonyl fluoride, supplemented with 1% Triton X-100) by pipetting and incubated for 30 min on ice. The cell lysates were centrifuged at 15,000 × *g* for 20 min, and the supernatant fluid was collected. The protein concentration in each sample was quantified and normalized by adding immunoprecipitation buffer. An aliquot of the lysate was saved at this step as the input fraction. Cell lysates were precleared with 30 µl of protein G (50% slurry) for 30 min at 4°C, and the resultant lysates were again incubated with 0.5 µg of anti-GS28 antibodies and 30 µl of protein G for 2.5 h with rotating at 4°C. The immunoprecipitated complex was washed three times with 1 ml of IP buffer, mixed with 60 µl of 2 × SDS sample buffer (100 mM Tris-HCl, pH 6.8, 4% SDS, 20% glycerol, 10% 2-mercaptoethanol, and 0.01% bromophenol blue), and boiled at 95°C for 5 min. After centrifugation to precipitate the beads, the supernatant fraction was used for subsequent experiments.

Assay for ACAT activity

ACAT activity in the cells was determined by measuring the incorporation of [^{14}C]oleic acid (American Radiolabeled Chemicals, St. Louis, MO) into cellular cholesteryl esters. Briefly, [^{14}C]oleic acid/BSA complex was prepared as previously described (Goldstein *et al.*, 1983) and added to a final concentration of 3 µCi/ml. After the incubation for 2 h, the cells were harvested as mentioned, and the lipids were extracted by the method of Bligh and Dyer (Bligh and Dyer, 1959). The lipids were then subjected to TLC on a Silica Gel 60 plate (Merck, Billerica, MA) using a mobile phase of petroleum ether/ethyl ether/acetic acid (60:40:1 [vol/vol/vol]). Distribution of radioactivity on the plate was quantified with a BAS1500 bioimaging analyzer (Fujix, Tokyo, Japan).

Pulse chase assay

The pulse chase assay was performed essentially as described previously (Saito *et al.*, 2009). Control or OSBP siRNA–treated HeLa cells were cultured in DMEM without methionine and cysteine (GIBCO) for 1 h and then pulsed with 77 µCi of [^{35}S]methionine for 15 min. Cells were washed and chased for 0, 1, or 3 h in DMEM containing 10 mM cold methionine. Medium was collected and precipitated with trichloroacetic acid. The sample was resolved by SDS–PAGE, followed by autoradiography. For brefeldin A treatment, 5 µg/ml brefeldin A was used throughout the experiments.

Statistics

Statistical analyses were performed with Student's *t* test, setting the significance at $p < 0.05$.

ACKNOWLEDGMENTS

We are grateful to Kenji Kontani (University of Tokyo, Tokyo, Japan) and Kumiko Ishii and Toshihide Kobayashi (RIKEN, Wako, Japan) for comments on the manuscript; Kota Saito (University of Tokyo) for help with the pulse chase assay; and Ikuyo Ichi (Ochanomizu University, Tokyo, Japan) for help with gas chromatography analysis. This work was supported by the Core Research for Evolutional Science and Technology, Japan Science and Technology Agency (H.A. and T.T.) and the Program for Promotion of Basic and Applied Researches for Innovations in Bio-oriented Industry (H.A.). T.N. is supported by a Japan Society for the Promotion of Science Research Fellowship and the Naito Foundation. V.L. is supported by the National Science Foundation (MCB-0645163) and the National Institutes of Health (1R01GM083144-01A1).

REFERENCES

Asp L *et al.* (2009). Early stages of Golgi vesicle and tubule formation require diacylglycerol. Mol Biol Cell 20, 780–790.

Banerji S, Ngo M, Lane CF, Robinson CA, Minogue S, Ridgway ND (2010). Oxysterol binding protein-dependent activation of sphingomyelin synthesis in the Golgi apparatus requires phosphatidylinositol 4-kinase IIalpha. Mol Biol Cell 21, 4141–4150.

Bligh EG, Dyer WJ (1959). A rapid method of total lipid extraction and purification. Can J Biochem Physiol 37, 911–917.

Churchward MA, Rogasevskaia T, Hofgen J, Bau J, Coorssen JR (2005). Cholesterol facilitates the native mechanism of Ca2+-triggered membrane fusion. J Cell Sci 118, 4833–4848.

Cubells L *et al.* (2007). Annexin A6-induced alterations in cholesterol transport and caveolin export from the Golgi complex. Traffic 8, 1568–1589.

Dawson PA, Ridgway ND, Slaughter CA, Brown MS, Goldstein JL (1989). cDNA cloning and expression of oxysterol-binding protein, an oligomer with a potential leucine zipper. J Biol Chem 264, 16798–16803.

Du X, Kumar J, Ferguson C, Schulz TA, Ong YS, Hong W, Prinz WA, Parton RG, Brown AJ, Yang H (2011). A role for oxysterol-binding protein-related protein 5 in endosomal cholesterol trafficking. J Cell Biol 192, 121–135.

Fairn GD, McMaster CR (2008). Emerging roles of the oxysterol-binding protein family in metabolism, transport, and signaling. Cell Mol Life Sci 65, 228–236.

Glick BS, Nakano A (2009). Membrane traffic within the Golgi apparatus. Annu Rev Cell Dev Biol 25, 113–132.

Goldstein JL, Basu SK, Brown MS (1983). Receptor-mediated endocytosis of low-density lipoprotein in cultured cells. Methods Enzymol 98, 241–260.

Goto A, Liu X, Robinson CA, Ridgway ND (2012). Multisite phosphorylation of oxysterol-binding protein regulates sterol binding and activation of sphingomyelin synthesis. Mol Biol Cell 23, 3624–3635.

Hay JC, Chao DS, Kuo CS, Scheller RH (1997). Protein interactions regulating vesicle transport between the endoplasmic reticulum and Golgi apparatus in mammalian cells. Cell 89, 149–158.

Im YJ, Raychaudhuri S, Prinz WA, Hurley JH (2005). Structural mechanism for sterol sensing and transport by OSBP-related proteins. Nature 437, 154–158.

Incardona JP, Roelink H (2000). The role of cholesterol in Shh signaling and teratogen-induced holoprosencephaly. Cell Mol Life Sci 57, 1709–1719.

Keller RK, Arnold TP, Fliesler SJ (2004). Formation of 7-dehydrocholesterol-containing membrane rafts in vitro and in vivo, with relevance to the Smith-Lemli-Opitz syndrome. J Lipid Res 45, 347–355.

Klemm RW *et al.* (2009). Segregation of sphingolipids and sterols during formation of secretory vesicles at the *trans*-Golgi network. J Cell Biol 185, 601–612.

Kobuna H, Inoue T, Shibata M, Gengyo-Ando K, Yamamoto A, Mitani S, Arai H (2010). Multivesicular body formation requires OSBP-related proteins and cholesterol. PLoS Genet 6, e1001055.

Kornfeld R, Kornfeld S (1985). Assembly of asparagine-linked oligosaccharides. Annu Rev Biochem 54, 631–664.
Lang T, Bruns D, Wenzel D, Riedel D, Holroyd P, Thiele C, Jahn R (2001). SNAREs are concentrated in cholesterol-dependent clusters that define docking and fusion sites for exocytosis. EMBO J 20, 2202–2213.
Lange Y, Steck TL (1997). Quantitation of the pool of cholesterol associated with acyl-CoA:cholesterol acyltransferase in human fibroblasts. J Biol Chem 272, 13103–13108.
Lanoix J, Ouwendijk J, Stark A, Szafer E, Cassel D, Dejgaard K, Weiss M, Nilsson T (2001). Sorting of Golgi resident proteins into different subpopulations of COPI vesicles: a role for ArfGAP1. J Cell Biol 155, 1199–1212.
Levine TP, Munro S (2002). Targeting of Golgi-specific pleckstrin homology domains involves both PtdIns 4-kinase-dependent and -independent components. Curr Biol 12, 695–704.
Linetti A, Fratangeli A, Taverna E, Valnegri P, Francolini M, Cappello V, Matteoli M, Passafaro M, Rosa P (2010). Cholesterol reduction impairs exocytosis of synaptic vesicles. J Cell Sci 123, 595–605.
Loewen CJ, Roy A, Levine TP (2003). A conserved ER targeting motif in three families of lipid binding proteins and in Opi1p binds VAP. EMBO J 22, 2025–2035.
Mellman I, Warren G (2000). The road taken: past and future foundations of membrane traffic. Cell 100, 99–112.
Mesmin B, Maxfield FR (2009). Intracellular sterol dynamics. Biochim Biophys Acta 1791, 636–645.
Mohammadi A, Perry RJ, Storey MK, Cook HW, Byers DM, Ridgway ND (2001). Golgi localization and phosphorylation of oxysterol binding protein in Niemann-Pick C and U18666A-treated cells. J Lipid Res 42, 1062–1071.
Nagahama M, Orci L, Ravazzola M, Amherdt M, Lacomis L, Tempst P, Rothman JE, Sollner TH (1996). A v-SNARE implicated in intra-Golgi transport. J Cell Biol 133, 507–516.
Ngo MH, Colbourne TR, Ridgway ND (2010). Functional implications of sterol transport by the oxysterol-binding protein gene family. Biochem J 429, 13–24.
Ngo M, Ridgway ND (2009). Oxysterol binding protein-related protein 9 (ORP9) is a cholesterol transfer protein that regulates Golgi structure and function. Mol Biol Cell 20, 1388–1399.
Nishimura T, Inoue T, Shibata N, Sekine A, Takabe W, Noguchi N, Arai H (2005). Inhibition of cholesterol biosynthesis by 25-hydroxycholesterol is independent of OSBP. Genes Cells 10, 793–801.
Oka T, Ungar D, Hughson FM, Krieger M (2004). The COG and COPI complexes interact to control the abundance of GEARs, a subset of Golgi integral membrane proteins. Mol Biol Cell 15, 2423–2435.
Pelham HR, Rothman JE (2000). The debate about transport in the Golgi—two sides of the same coin? Cell 102, 713–719.
Perry RJ, Ridgway ND (2006). Oxysterol-binding protein and vesicle-associated membrane protein-associated protein are required for sterol-dependent activation of the ceramide transport protein. Mol Biol Cell 17, 2604–2616.
Pol A, Martin S, Fernandez MA, Ingelmo-Torres M, Ferguson C, Enrich C, Parton RG (2005). Cholesterol and fatty acids regulate dynamic caveolin trafficking through the Golgi complex and between the cell surface and lipid bodies. Mol Biol Cell 16, 2091–2105.
Porter FD, Herman GE (2011). Malformation syndromes caused by disorders of cholesterol synthesis. J Lipid Res 52, 6–34.
Raychaudhuri S, Im YJ, Hurley JH, Prinz WA (2006). Nonvesicular sterol movement from plasma membrane to ER requires oxysterol-binding protein-related proteins and phosphoinositides. J Cell Biol 173, 107–119.
Raychaudhuri S, Prinz WA (2010). The diverse functions of oxysterol-binding proteins. Annu Rev Cell Dev Biol 26, 157–177.
Ridgway ND, Dawson PA, Ho YK, Brown MS, Goldstein JL (1992). Translocation of oxysterol binding protein to Golgi apparatus triggered by ligand binding. J Cell Biol 116, 307–319.
Saito K, Chen M, Bard F, Chen S, Zhou H, Woodley D, Polischuk R, Schekman R, Malhotra V (2009). TANGO1 facilitates cargo loading at endoplasmic reticulum exit sites. Cell 136, 891–902.
Shestakova A, Suvorova E, Pavliv O, Khaidakova G, Lupashin V (2007). Interaction of the conserved oligomeric Golgi complex with t-SNARE Syntaxin5a/Sed5 enhances intra-Golgi SNARE complex stability. J Cell Biol 179, 1179–1192.
Simons K, Gerl MJ (2010). Revitalizing membrane rafts: new tools and insights. Nat Rev Mol Cell Biol 11, 688–699.
Sollner T, Whiteheart SW, Brunner M, Erdjument-Bromage H, Geromanos S, Tempst P, Rothman JE (1993). SNAP receptors implicated in vesicle targeting and fusion. Nature 362, 318–324.
Stuven E, Porat A, Shimron F, Fass E, Kaloyanova D, Brugger B, Wieland FT, Elazar Z, Helms JB (2003). Intra-Golgi protein transport depends on a cholesterol balance in the lipid membrane. J Biol Chem 278, 53112–53122.
Tanigawa G, Orci L, Amherdt M, Ravazzola M, Helms JB, Rothman JE (1993). Hydrolysis of bound GTP by ARF protein triggers uncoating of Golgi-derived COP-coated vesicles. J Cell Biol 123, 1365–1371.
Taylor FR, Saucier SE, Shown EP, Parish EJ, Kandutsch AA (1984). Correlation between oxysterol binding to a cytosolic binding protein and potency in the repression of hydroxymethylglutaryl coenzyme A reductase. J Biol Chem 259, 12382–12387.
Tong J, Borbat PP, Freed JH, Shin YK (2009). A scissors mechanism for stimulation of SNARE-mediated lipid mixing by cholesterol. Proc Natl Acad Sci USA 106, 5141–5146.
van Meer G (1989). Lipid traffic in animal cells. Annu Rev Cell Biol 5, 247–275.
Vihervaara T, Jansen M, Uronen RL, Ohsaki Y, Ikonen E, Olkkonen VM (2011). Cytoplasmic oxysterol-binding proteins: sterol sensors or transporters? Chem Phys Lipids 164, 443–450.
Wyles JP, McMaster CR, Ridgway ND (2002). Vesicle-associated membrane protein-associated protein-A (VAP-A) interacts with the oxysterol-binding protein to modify export from the endoplasmic reticulum. J Biol Chem 277, 29908–29918.
Xu Y, Martin S, James DE, Hong W (2002). GS15 forms a SNARE complex with syntaxin 5, GS28, and Ykt6 and is implicated in traffic in the early cisternae of the Golgi apparatus. Mol Biol Cell 13, 3493–3507.
Yang JS, Lee SY, Gao M, Bourgoin S, Randazzo PA, Premont RT, Hsu VW (2002). ARFGAP1 promotes the formation of COPI vesicles, suggesting function as a component of the coat. J Cell Biol 159, 69–78.
Yang JS, Zhang L, Lee SY, Gad H, Luini A, Hsu VW (2006). Key components of the fission machinery are interchangeable. Nat Cell Biol 8, 1376–1382.
Ying M, Grimmer S, Iversen TG, Van Deurs B, Sandvig K (2003). Cholesterol loading induces a block in the exit of VSVG from the TGN. Traffic 4, 772–784.
Zolov SN, Lupashin VV (2005). Cog3p depletion blocks vesicle-mediated Golgi retrograde trafficking in HeLa cells. J Cell Biol 168, 747–759.